Supporting Information for

Probing Absolute Spin Polarization at the Nanoscale

Matthias Eltschka,[1,*] Berthold Jäck,[1] Maximilian Assig,[1] Oleg V. Kondrashov,[2]
Mikhail A. Skvortsov,[3,4,2] Markus Etzkorn,[1] Christian R. Ast,[1] and Klaus Kern[1,5]

[1]*Max-Planck-Institut für Festkörperforschung, 70569 Stuttgart, Germany*

[2]*Moscow Institute of Physics and Technology, 141700 Moscow, Russia*

[3]*Skolkovo Institute of Science and Technology, 143025 Skolkovo, Russia*

[4]*L. D. Landau Institute for Theoretical Physics, 142432 Chernogolovka, Russia*

[5]*Institut de Physique de la Matière Condensée,*
Ecole Polytechnique Fédérale de Lausanne, 1015 Lausanne, Switzerland

(Dated: November 28, 2014)

I. MESERVEY-TEDROW-FULDE TECHNIQUE

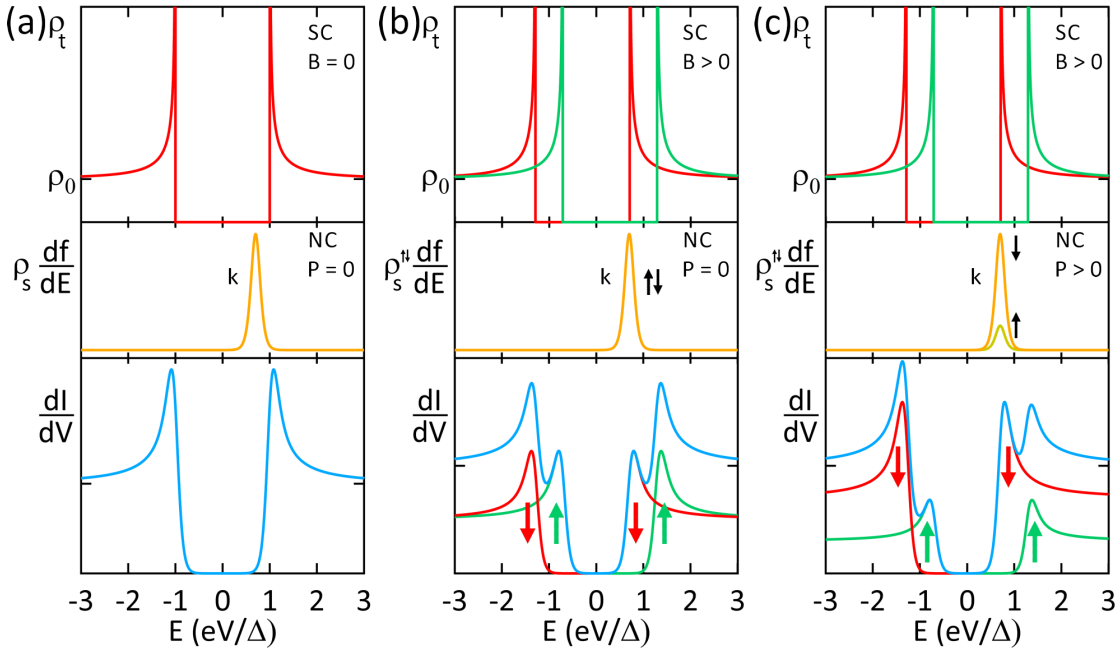

FIG. S1: Origin of the differential conductance (dI/dV) spectra used in the Meservey-Tedrow-Fulde technique.[S1–S3] This technique employs tunneling experiments between a superconductor (SC) and a normal conducting (NC) electrode separated by an insulating layer. The figure is based on Fig. 1-3 of Ref. S3. The top panel always depicts the quasi-particle density of states (DOS) of the SC. (In our case, ρ_t is the DOS of the superconducting tip). The middle panel describes thermal broadening as well as the two contributions of the spin-up DOS ($\rho_s^{\uparrow}$) and spin-down DOS ($\rho_s^{\downarrow}$) of the normal conducting electrode. The resulting dI/dV spectrum is shown in the bottom panel. (a) The quasi-particle DOS of the SC ρ_t exhibits a characteristic gap and two coherence peaks (top). The derivative k of the Fermi function $f(E)$ takes into account thermal broadening effects (middle). The measured dI/dV spectrum is the result of convolving the quasi-particle DOS and derivative of the Fermi function (bottom). (b) In an external magnetic field the quasi-particle DOS is split by the Zeeman energy and four peaks are observed in the dI/dV spectrum. (c) For a ferromagnetic electrode a spin polarization at the Fermi level leads to an imbalance between spin-up and spin-down electrons. The spin polarization of the tunneling electrons can be directly extracted from the asymmetry of the dI/dV spectrum.

In their pioneering work Meservey and Tedrow employed tunneling experiments between a

superconductor (SC) and a normal conducting (NC) electrode separated by an insulating layer to reveal detailed information about the quasi-particle density of states (DOS).[S1] For single electrons to tunnel, a Cooper pair has to break which requires an energy Δ. The resulting quasi-particle DOS shows a characteristic gap (Fig. S1(a)). The differential conductance (dI/dV) measured between the SC and the NC is thermally broadened by the Fermi edge of the metal. This is taken into account by convolving the superconducting quasi-particle DOS and the derivative of the Fermi function (Fig. S1(a)). In magnetic fields B, the spin degeneracy of the quasi-particle DOS is lifted by the Zeeman energy into a spin-up and a spin-down channel that are separated by $E/B = 2\mu_B \approx 116\ \mu\mathrm{eV/T}$ for $s = 1/2$, g-factor $= 2$ and μ_B the Bohr magneton (Fig. S1(b)). If the normal conducting metal of the tunnel junction is non-magnetic, the contributions of the spin-up and the spin-down channel are equivalent that results in a symmetric dI/dV spectrum. In the case of a ferromagnetic sample, however, the DOS typically differs between spin-up and spin-down channel (Fig. S1(c)). Since the measured dI/dV spectrum is the sum of spin-up and spin-down channels, the spin-polarization of the ferromagnetic electrode at the Fermi energy results in an asymmetric dI/dV spectrum. Analyzing the asymmetric dI/dV spectrum reveals absolute values of the spin-polarization at Fermi energy.[S2,S3] For these experiments, it is essential that the Zeeman splitting exceeds the thermal broadening. This is best achieved by increasing the critical magnetic fields of superconductors, for example, due to geometrical confinement in thin films. If the thickness of these superconducting layers decreases below the London penetration depth compensating currents cannot be formed efficiently anymore in external magnetic fields and, as result, the critical fields exceed the critical bulk fields.[S4] As discussed below, the similar situation occurs in the apex of the used superconducting STM tips

II. EXPERIMENTAL METHODS

Our measurements are carried out in a scanning tunneling microscope (STM) operating in ultra-high vacuum (UHV) at $15\ \mathrm{mK}$ temperature.[S5] External magnetic fields up to $14\ \mathrm{T}$ can be applied perpendicular to the sample plane.[S5] An UHV preparation chamber attached to the system allows for the sample and tip preparation as well as the transfer to the STM unit *in situ*. The V(100) (Cu(111)) sample is cleaned in several cycles of Ar^+ ion sputtering and annealing to $\approx 1000\ ^\circ\mathrm{C}$ ($\approx 600\ ^\circ\mathrm{C}$) for several minutes. On Cu(111), Co is deposited in sub-monolayer coverage at room temperature by using an electron beam evaporator. In this regime, Co forms bilayer islands of

triangular shape. After being transferred to the STM unit without breaking the UHV, the samples are cooled down for the measurements. STM tips are mechanically cut under tension from polycrystalline V wire of $99.8\ \%$ purity and are transferred to the STM unit as well. The thin native oxide is removed by field emission on the V(100) sample. After such a preparation all V tips are superconducting at $1\ \mathrm{K}$, however with strongly varying properties. In magnetic fields, the superconductivity of the tips is optimized by short bias voltage pulses to shape the tip apex on the V(100) sample. As soon as the tips show superconductivity at higher magnetic fields, the STM unit is cooled down to $15\ \mathrm{mK}$. At this temperature, differential conductance (dI/dV) spectra are acquired by lock-in technique (modulation amplitude $V_{\mathrm{mod}} = 20\ \mu\mathrm{V}$, modulation frequency $f_{\mathrm{mod}} = 720\ \mathrm{Hz}$). After stabilizing the tunneling contact at I_S and V_S the feedback loop is opened and the dI/dV spectra are measured as function of the bias voltage. Contrary to the ferromagnetic tips typically used in SP-STM, the superconducting tip apex does not possess a magnetic moment and the DOS of the superconductor is spin-independent for energies outside the gap region ($E \gg \Delta$). Thus, for $eV_S \gg \Delta$ the tunnel contact can be stabilized at the same conditions regardless of the possible variations of the spin polarization of the sample. The measured spin polarization as well as variations of the spin polarization can solely be traced back to the sample. For the Cu(111) substrate with the Co nanoislands, no significant difference of the superconducting gap is found between measurements on the Co island and the Cu(111) substrate. This indicates that the superconducting tip is not affected by the Co in vicinity. We conclude that the weak stray field of the thin Co nanoisland does not significantly influence the superconducting tip with the characteristic length scale of approximately the London penetration depth. Further, we do not observe any influence of an induced magnetic tip moment due to the Meissner screening.

III. MAKI THEORY

The dI/dV spectra are analyzed by a fitting routine based on Maki's theory[S6,S7] where the superconducting DOS is given by

$$\rho_{\downarrow\uparrow}(E) = \frac{\rho_0}{2}\,\mathrm{sign}\,(E)\ \mathrm{Re}\left(\frac{u_\pm}{\sqrt{u_\pm^2 - 1}}\right) \tag{1}$$

with u_+ and u_- are implicitly defined as

$$u_\pm = \frac{E \mp \mu B}{\Delta} + \zeta\,\frac{u_\pm}{\sqrt{1-u_\pm^2}} + b\,\frac{u_\mp - u_\pm}{\sqrt{1-u_\mp^2}} \tag{2}$$

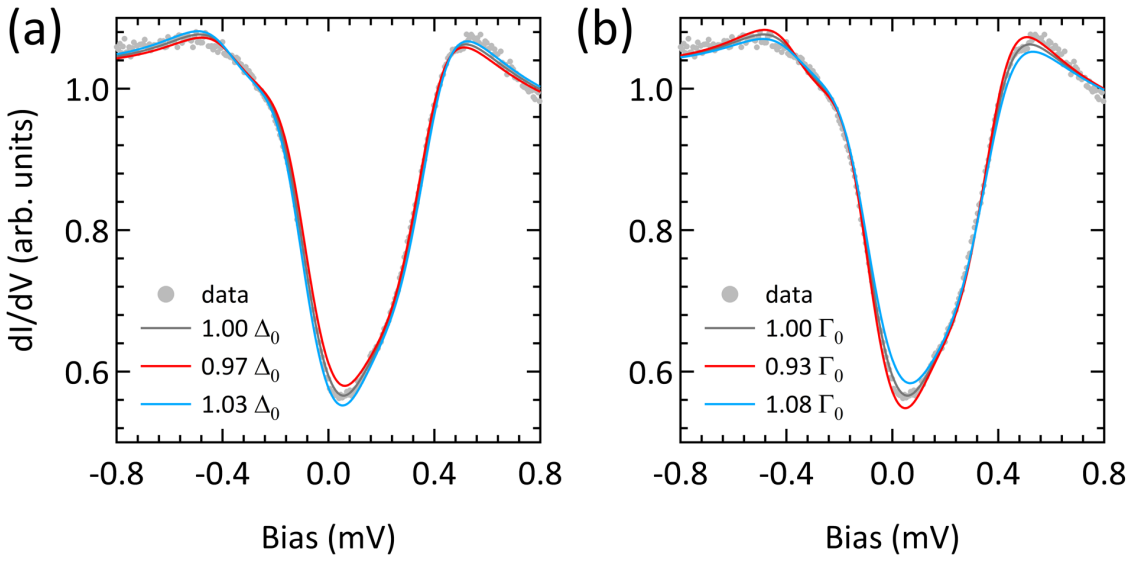

FIG. S2: Error estimation for our fitting routine (example dI/dV spectrum with 54 % spin polarization). (a) The superconducting gap Δ is increased, respectively decreased, by 3 % and the fitting routine is run to optimize dI/dV by varying P. (b) dI/dV spectra are optimized for increased, respectively decreased, damping parameter Γ.

with ρ_0 the normal conducting DOS, E the energy ($E_F = 0$), μ the magnetic moment, Δ the superconducting energy gap, ζ the orbital depairing parameter, B the external magnetic field and b is the spin-orbit scattering parameter. Since Maki's theory does not consider the confinement of STM tips, an additional damping parameter according to Dynes is included by $E \rightarrow E - i\Gamma$[S8] to phenomenologically take into account diamagnetic effects due to the specific tip geometry. The final expression of our fitting function includes the spin polarization of the tunneling electrons P and thermal broadening described by the derivative of the Fermi function $f'(E)$ at temperature T:

$$\frac{dI}{dV} \propto \frac{1+P}{2} \int_{-\infty}^{+\infty} \rho_{\uparrow}(E,B)\, f'(E+eV,T)\, dE + \frac{1-P}{2} \int_{-\infty}^{+\infty} \rho_{\downarrow}(E,B)\, f'(E+eV,T)\, dE \quad (3)$$

Additionally, we correct small known bias offsets in the dI/dV spectra and subtract a linear background. In general, the fits based on Eq. 3 converge for all of our acquired dI/dV spectra and are used to extract the spin polarization of the tunneling electrons. The resulting spin polarization is found to be influenced by the other fitting parameters. From the fits of the dI/dV spectra obtained on Cu we obtain the spin-orbit coupling $b = 0.14$. Since this value is in good agreement with experiments carried out on thin film sandwich junctions[S9] we keep the spin-orbit parameter

constant in our fitting routine. For the orbital depairing parameter, we achieve the best fits on Cu for $\zeta = 0.05$ which we also keep constant. Then, the spin polarization is mainly influenced by Δ and Γ and, therefore, we focus on these two parameters in our error estimation. To estimate this error, we vary a single fitting parameter (such as Δ) so that it deviates on purpose from the ideal fitting value. Keeping this parameter fixed we run the fitting routine and evaluate the resulting spin polarization. In Fig. S2(a), Δ is fixed to a value increased, respectively decreased, by $3\ \%$ from the best fitting result (Δ_0) and the fitting routine is run to optimize P. Even these small deviations significantly alter the resulting dI/dV spectra and the quality of the fits is critically decreased (χ^2 increases by six orders of magnitude). The resulting spin polarization is increased, respectively decreased, by $1\ \%$. In Fig. S2(b), we vary Γ similar to the previous calculations for Δ (χ^2 increases in the same range). The resulting spin polarization is changed by $\pm 5\ \%$. Considering the good agreement between our fits and the experimental data, we can regard the deviations discussed in Fig. S2 as the upper limit. Assuming negligible correlation between Δ and Γ, we calculate the total error propagation of the spin polarization which leads to the error estimation given in the main article.

IV. USADEL EQUATION IN THE TIP

The detailed correlation between geometrical confinement and superconductivity in high magnetic fields has been well-studied over the last decades.[S4,S10] To obtain a better understanding of the non-uniform superconducting state in the V tip, we employ the Usadel equation[S11] appropriate in the dirty limit. If the magnetic field B is applied along the tip axis (z-direction), the Usadel equation for spin-down quasi-particles can be written in terms of the spectral angle $\theta_\epsilon(\mathbf{r})$,[S12] where ϵ is the imaginary (Matsubara) energy. For sharp tips, one can employ the adiabatic approximation neglecting variations perpendicular to the cone axis. The resulting equation for the function $\theta_\epsilon(z)$ can be written as:

$$\frac{\hbar D}{2}\left[-\theta_\epsilon'' - \frac{2R'(z)}{R(z)}\theta_\epsilon' + \left(\frac{\pi B}{2\Phi_0}\right)^2 R^2(z)\sin 2\theta_\epsilon\right] + (\epsilon - i\mu B)\sin\theta_\epsilon = \Delta(z)\cos\theta_\epsilon, \qquad (4)$$

where the conical tip surface is described by the equation $R(z) = \alpha z$ (α is the opening angle), $D = v_F l/3$ is the diffusion coefficient (v_F is the Fermi velocity and l is the mean free path), $\Phi_0 = hc/2e$ is the superconducting flux quantum, and μ is the magnetic moment. The order parameter field $\Delta(z)$ is a function of z along the tip axis and should be determined from the

self-consistency equation. At $T = 0$ the latter takes the form

$$\frac{\Delta(z)}{\lambda} = \mathrm{Re}\int_0^{\hbar\omega_D} \sin\theta_\epsilon(z)\, d\epsilon, \tag{5}$$

where λ is electron-phonon coupling constant, and ω_D is the Debye frequency. The DOS (normalized by the normal-metal DOS) at a real energy E is obtained by analytic continuation $\epsilon \to iE$:

$$\rho_{\downarrow\uparrow}(E, z) = 1/2\, \rho_0\, \mathrm{sign}(E)\, \mathrm{Re}\cos\theta^{\pm}_{iE}(z), \tag{6}$$

where $\theta^+ = \theta$, and θ^- is obtained by changing the sign of B.

Following this approach we can correlate the opening angle α with the critical fields and the broadening observed in the dI/dV spectra of the V tips. Wider tip geometries (larger α) result in lower critical fields and the dI/dV spectra generally appear more broadened. Our model calculations have shown that the effects of the tip geometry can be well approximated by the phenomenological parameter Γ in the Maki equation. We note that Eq. 4 is the generalization of the Maki theory to a non-uniform case. This can easily be seen from comparing Eq. 1 with Eq. 6 and the relation $u_\pm = -i\coth\theta^\pm$. As the self consistency calculation is very time consuming, it has not been included in our fitting routine. Instead, to determine the spin-polarization, we have decided to use the much simpler Maki equation discussed above.[S6,S7]

V. 1D MODEL FOR CO NANOISLAND

When measuring the spin polarization of the tunneling electrons on the Co nanoisland, we find that the spin polarization also depends on the tip-to-sample distance. For the same position on a Co nanoisland, two representative dI/dV spectra are presented in Fig. S3. From these dI/dV spectra we extract 34 ± 3 % spin polarization at higher conductance and 56 ± 5 % spin polarization for lower conductance.

A simple one dimensional model is utilized to describe the spin polarization as function of the conductance. The spin polarization P of the tunnel current I is calculated from

$$P = \frac{I_\uparrow - I_\downarrow}{I_\uparrow + I_\downarrow}. \tag{7}$$

In this simplified model the spin-up ($I_\uparrow$) and spin-down ($I_\downarrow$) contributions of the tunnel current are given by

$$I_{\uparrow\downarrow} \propto |\langle\psi_{\uparrow\downarrow}|\psi_{\mathrm{tip}}\rangle|^2 \tag{8}$$

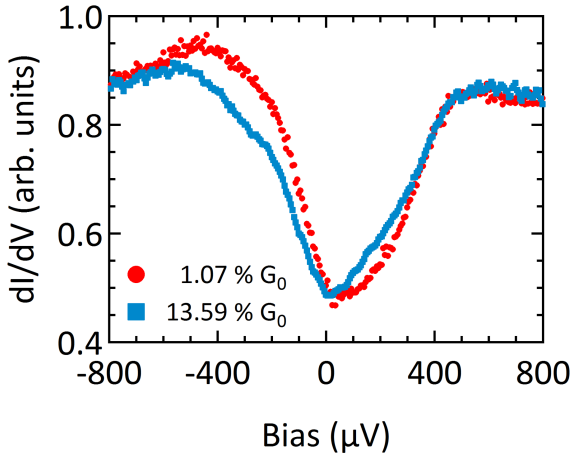

FIG. S3: dI/dV tunnel spectra acquired with a superconducting V tip on a Co island. At higher conductance the dI/dV spectrum is less asymmetric due to a lower spin polarization (P $= 34 \pm 3$ %) than at lower conductance (P $= 56 \pm 5$ %) ($V_S = 9.5$ mV).

with the majority (minority) Co state $\psi_\uparrow$ ($\psi_\downarrow$) and the electronic state of the V tip ψ_{tip}. Here, the tunnel current only depends on the overlap of the electronic states.

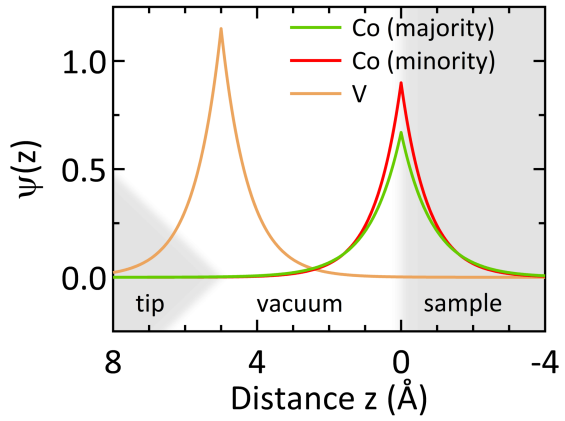

FIG. S4: 1D model for distance dependence of the spin polarization. In this 1D model, the overlap as function of distance is calculated for the Co minority and majority states with the exponentially decaying state of the tip.

The decay of the wave functions into vacuum is modeled by exponential functions in the form of $\psi_{\mathrm{out}}(z) = \alpha e^{-\beta|z|}$ (Fig. S4). For the Co majority state we use the vacuum wave vector $k_0 = \sqrt{2m_0\Phi/\hbar^2}$ with the free electron mass m_0 and the work function for Co $\Phi = 5$ eV.[S13,S14] The

minority state is modeled with a wave vector that reproduces the spin polarizations of $\mathrm{P} = -3\ \%$ ($\mathrm{P} = 34\ \%$) at 2.08 Å (4.16 Å) above the Co island as found in DFT calculations.[S15]

VI. DISTANCE DEPENDENCE OF THE CURRENT

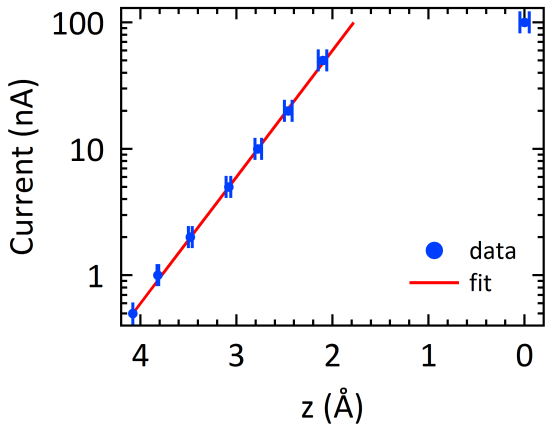

FIG. S5: Distance dependence of the tunnel current. The tunnel current increases exponentially when the tip-to-sample distance is decreased proofing that the measurements apart from the last point are taken in the tunneling regime ($V_S = 9.5$ mV).

When measuring the distance dependence of the spin polarization we reduce the tip-to-sample distance. Here, we demonstrate that our measurements are still carried out in the tunneling regime and effects due to the transition to the point contact regime can be neglected. For the stabilizing conditions ($V_S = 9.5$ mV), the tunnel current is shown as function of the distance z in Fig. S5 (z-values are drift corrected). For all except the last data point in our investigated conductance range, the tunnel current I follows an exponential law with the decay constant $\alpha = 2.3$ Å^{-1}. As expected for the tunneling regime, the current decreases by an order of magnitude when the tunneling distance is increased by 1 Å. Since the tunnel current follows this exponential law, we only need to consider the width of the tunnel barrier in our theoretical 1D description. Changes in the barrier height Φ are negligible. This is an important finding, since it means that the electron wave vector in the barrier κ is constant ($\kappa \propto \sqrt{\Phi}$). Therefore, the distance dependence of the spin polarization is not the result of the varying electron momentum as described by the Slonczewski model.[S16,S17]

* Corresponding author; electronic address: m.eltschka@fkf.mpg.de

[S1] Meservey, R.; Tedrow, P. M.; Fulde, P. *Phys. Rev. Lett.* **1970**, *25*, 1270–1272.

[S2] Tedrow, P. M.; Meservey, R. *Phys. Rev. Lett.* **1971**, *26*, 192–195.

[S3] Tedrow, P. M.; Meservey, R. *Phys. Rev. B* **1973**, *7*, 318–326.

[S4] Meservey, R.; Douglass, D. H. *Phys. Rev.* **1964**, *135*, A24–A33.

[S5] Assig, M.; Etzkorn, M.; Enders, A.; Stiepany, W.; Ast, C. R.; Kern, K. *Rev. Sci. Instrum.* **2013**, *84*, 033903.

[S6] Maki, K. *Prog. Theor. Phys.* **1964**, *32*, 29.

[S7] Worledge, D. C.; Geballe, T. H. *Phys. Rev. B* **2000**, *62*, 447–451.

[S8] Dynes, R. C.; Narayanamurti, V.; Garno, J. P. *Phys. Rev. Lett.* **1978**, *41*, 1509–1512.

[S9] Tedrow, P.; Meservey, R. *Phys. Lett. A* **1978**, *69*, 285 – 286.

[S10] Chen, Y.; Doria, M. M.; Peeters, F. M. *Phys. Rev. B* **2008**, *77*, 054511.

[S11] Usadel, K. D. *Phys. Rev. Lett.* **1970**, *25*, 507–509.

[S12] Ivanov, D.; Fominov, Ya. V.; Skvortsov, M. A.; Ostrovsky, P. M. *Phys. Rev. B* **2009**, *80*, 134501.

[S13] Davison, S. G.; Steslicka, M. *Basic Theory of Surface States*; Clarendon Press, 1996.

[S14] Tipler, P. A.; Llewellyn, R. A. *Modern Physics*; W.H. Freeman, 1999.

[S15] Ignatiev, P. Theoretical study of spin-polarized surface states on metal surfaces. Ph.D. thesis, 2009.

[S16] Slonczewski, J. C. *Phys. Rev. B* **1989**, *39*, 6995.

[S17] Gimzewski, J. K.; Möller, R. *Phys. Rev. B* **1987**, *36*, 1284.